PECULIARITIES OF GLOW MODES OF ARGON ATMOSPHERIC PRESSURE RADIO-FREQUENCY CAPACITIVE DISCHARGE WITH ISOLATED ELECTRODES

V.Yu. Bazhenov[1], V.V. Tsiolko[1], V.M. Piun[1], R.Yu. Chaplinskiy[2], A.I. Kuzmichev[2]
[1]Institute of Physics NAS of Ukraine, Kiev, Ukraine;
[2]National Technical University of Ukraine "KPI", Kiev, Ukraine
E-mail: chapok86@ukr.net

Glow characteristics of capacitive radio frequency discharge with isolated electrodes in low-current α and high-current γ modes are determined experimentally. It is shown that transition from α mode to γ mode occurs through a phase of coexistence of both modes in different parts of the discharge gap.

PACS: 52.80.Pi, 61.30.Hn, 81.65.-b

INTRODUCTION

In past decade atmospheric pressure discharges were widely used in many applications, including sterilization, surface treatment, exhaust purification, nanoscience [1 - 3]. It should be noted that among a variety of such discharges (dielectric barrier discharges (DBDs), plasma jets, microwave discharges, radio-frequency (RF) discharges) the last kind is of the utmost interest. Advantages of such discharges are low ignition voltage and ability to create dense uniform plasma in large volumes. Capacitively coupled plasmas in such discharges usually are generated between bare metal electrodes typically at 13.56 MHz. As in case of low pressure discharges, atmospheric pressure ones can exist in two modes – low-current α mode, and high-currentp γ one [4]. Transition from α to γ mode occurs in result of "breakdown" of space charge layers of the discharge in α mode, which leads to contraction of the discharge, and at subsequent voltage growth arcing may occur in some cases. Due to that, in spite of higher efficiency of γ-mode discharge owing to its higher current density, the discharge instability becomes principal drawback in its practical applications.

In [5, 6] it was proposed to use dielectric barriers for stabilization of γ mode of RF discharge glow. Experimental and theoretical investigations of RF discharge with dielectric barriers in helium at atmospheric pressure confirmed possibility of stable operation of γ-mode discharge at high current values [7, 8].

However, in case of practical application of RF discharges, use of helium as main gas in different mixtures is not justified due to its high cost. In [9] for creation of layers for liquid crystal alignment, RF discharge with dielectric barriers in argon at atmospheric pressure was successfully used with operation in low-current α mode. The present paper represents results of experimental study of glow peculiarities of such discharge at its transition from low-current α mode to high-current γ mode.

1. EXPERIMENTAL SET UP AND METHODS

Block diagram of the experimental setup is presented in Fig. 1. Discharge cell consisted of two flat copper electrodes, each having 50×41×0.05 mm dimension, glued onto polycore (Al_2O_3) dielectric barriers 5 (60×48×1 mm). Discharge gap between barriers 5 had 1 mm thickness.

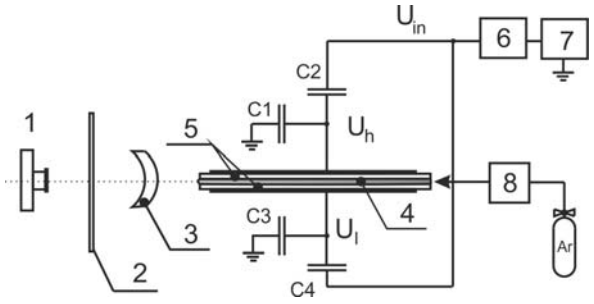

Fig. 1. Scheme of experimental setup. 1 – camera; 2 – color filter; 3 – lens; 4 – discharge plasma; 5 – dielectric barriers; 6 – impedance matching unit; 7 – RF generator; 8 – gas feed regulation system

For powering the discharge device, RF (13.56 MHz) generator 7 (MV-1.5, JSC "Selmi", Sumy) was used with impedance matching unit 6. Voltage RMS value after the matching unit could be varied in a range of 0…1600 V. The power was supplied to the electrodes via capacitive dividers (C1-C2, C3-C4) for setting desired ratio of RF voltage values between the discharge electrodes. Volume rate of argon feed υ was set in a range of 0.5…18 l/min by means of gas feed regulation system 8.

For studies of electrical characteristics of the discharge, capacitive bridge technique was implemented using the circuit shown in Fig. 1, with capacitors C1-C4 serving as the bridge components, and the discharge cell included as a diagonal element of the bridge. At that, kinetics of 3 RF oscillation periods for values of three voltages (U_{in}, U_h and U_l) were recorded by means of digital oscilloscope Tektronix TDS1012 and transferred to computer for subsequent processing. At first, current values through capacitors C1-C4 were calculated, and after that current values through the discharge cell from high-potential and low-potential sides were determined. It was found that in all cases of discharge cell use (that is, with discharge in different operating regimes, as well as without ignition of the discharge) high side cell current value was about 15% higher than low side one. At that, with discharge cell removed and shorted connection instead of it, measured current values were equal. Examination of the discharge cell capacity by means of low-frequency metering device (with the cell located in its actual experimental arrangement) has shown that additionally to 18 pF capacity of the cell itself (including the gap and two insulators, each of the dielectric

barrier introducing 180 pF capacity) there are leakage capacities of high side and low side electrodes with respect to grounded surrounding elements of the setup comprising 3 and 4 pF respectively (the vales measured with ±0.1 pF precision). Such situation obviously required taking into account actual leakage capacities at RF frequencies for correct determination of the discharge characteristics. It was done by processing the data with mentioned leakage capacities taken as starting values, and subsequent iterations with variation of the values so that the discharge current values calculated from high and low side became equal. The technique was calibrated for correct absolute value measurements by means of consequently connected RC circuits instead of the discharge cell with parameters simulating actual discharge operation. As a result, the technique allowed experimental determination of principal electrical characteristics (voltage, current, total power, active power, efficient capacity and resistance) of the gas discharge itself, that is, at the gas space between dielectric barriers.

Measurements of the discharge emission spectrum were performed by means of CCD-spectrometer SL40-2-1024USB (SOLAR TII, Minsk, Republic of Belarus). Emission distribution across the discharge was studied by means of long focal length system, which was implemented on a basis of DSLR camera Canon 350D with its own lens removed and single lens with claimed focal length of 1 m and 25 mm aperture installed at special rigid mount (actual magnification of the system was determined experimentally by the image processing). At that the necessity of correct imaging of the whole depth of the discharge in the cell (about 5 cm) was taken into consideration. Particularly, for studied red region of the spectrum centered at about 650 nm, Rayleigh length criterion allowed maximum possible optical resolution at the discharge cell location of about $\sqrt{5\cdot10^4\cdot0.65}$ μm ≈180 μm, and used distance between the lens and the discharge cell of about 4 m provided approximate match with the diffraction divergence. Images taken by the camera in RAW mode were converted to 16-bit bitmap files with linear law of intensity conversion so that they could be immediately used for obtaining profiles of discharge intensity distribution. Results presented in this paper were obtained with red filter with cutoff wavelength of about 600 nm installed before the camera. Other zones of visible spectra (green and blue) accepted by the camera have demonstrated similar behavior of spatial intensity distributions, however, with worse signal-to-noise ratio, as compared to red zone of visible spectrum.

2. EXPERIMENTAL RESULTS AND DISCUSSION

2.1. RESULTS OF THE ELECTRICAL MEASUREMENTS

At conducting the researches, the following values were determined experimentally: RMS values of discharge current density J_d and voltage at the discharge gap between dielectric barriers U_g (gas voltage), mean active discharge power W_d, and effective (averaged over RF oscillation period) values of gas space capacity C_g and active resistance of the discharge plasma R_d.

One can see from Fig. 2 that discharge ignition voltage U_{ign} is practically independent on volume rate of argon flow through the discharge gap. At the same time, discharge quenching voltage U_{quen} grows up from ≈ 60 to ≈ 110 V (that is, practically twice) at increase of argon flow rate υ from 1 to 12 l/min.

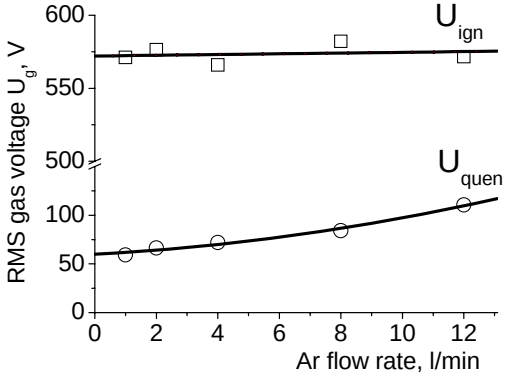

Fig. 2. Dependencies of voltage of discharge ignition U_{ign} and quenching U_{quen} on volume rate of argon flow υ. Each point at the plot represents data averaged over 15-20 measurements for each dataset

Possible reason for such effect may be due to plasma generation in the discharge not only at the expense of ionization of argon atoms in ground state, but as well at the expense of ionization of the atoms in metastable states $Ar(1p_5)$ and $Ar(1p_3)$. In discharges on argon-containing mixtures specific portion of metastable argon atoms Q (that is, ratio of concentration of metastable argon atoms to that of the atoms in ground state) can reach values of $10^{-5}…10^{-3}$ depending on discharge parameters and mixture content. Such quantity of metastable atoms can provide essential influence on kinetics of processes in discharge plasmas, since ionization of argon atoms from their metastable states can occur with high enough efficiency. It is due both to lower energy threshold of such processes, and to higher values of their cross sections. Particularly, cross section of argon atom ionization from ground state reaches maximum value of $\approx 3\cdot10^{-16}$ cm^2 (at 100 eV) with the process threshold of 15.8 eV, and maximum cross section for ionization from metastable state $1s_5 \approx 8\cdot10^{-16}$ cm^2 (at ≈ 15 eV) with the threshold of ≈ 4 eV [10, 11]. In [12] it was shown that in low pressure discharge, depending on parameters, contribution of ionization from metastable states can reach up to 20…25%. Contribution of metastable atoms to ionization increases with pressure growth. First of all, it is due to fact that decrease of electron energy with pressure growth leads to increase of contribution of "low energy" ionization from metastable states, as compared to "higher energy" ionization from ground state.

Figs. 3-5 present measured dependencies of main discharge parameters on RMS gas voltage U_g. One can see from Fig. 3 that behavior of discharge power W_d dependence on U_g is similar for both values of argon flow rate – initial slow (practically linear) W_d increase after $U_g \approx 210$ V is substituted by faster growth.

Similar behavior is also demonstrated by dependencies of gas space capacity C_g (see Fig. 4) dependence on flow rate is absent; b) at low values of U_g the capacity values are practically independent on U_g and start abrupt growth at $U_g \geq \approx 210$ V.

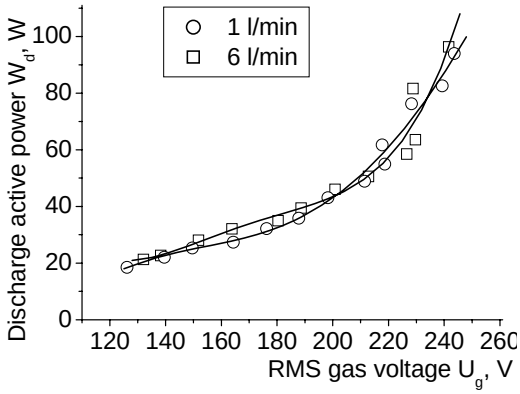

Fig. 3. Dependencies of active discharge power W_d on gas voltage U_g for different volume rates of argon flow

Possible reason of such behavior of C_g dependence on U_g may consist in change of the discharge glow mode at increase of the voltage value above ≈ 210 V. At discharge glow in α mode, thicknesses of space charge layers (and, consequently, gas space capacity C_g) are practically independent on U_g. Breakdown of space charge layers in α-mode discharge at increase of voltage U_g above certain threshold (≈ 210 V in the above case) leads to abrupt decrease of thickness of the layers and, consequently, to rapid growth of gas space capacity C_g. Thus, rapid increase of C_g observed in the experiment gives evidence to transition (total or partial) of discharge glow from α mode to high-current γ mode.

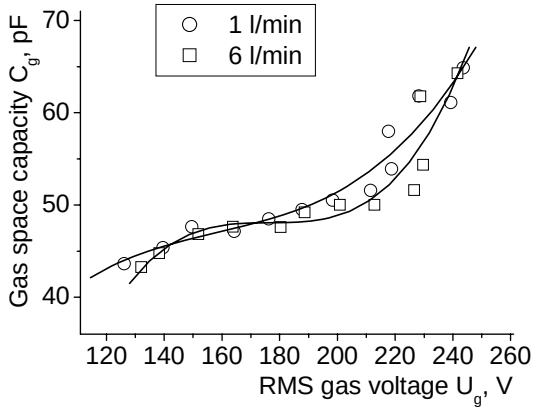

Fig. 4. Dependencies of discharge gas space capacity C_g on gas voltage U_g for different volume rates of argon flow

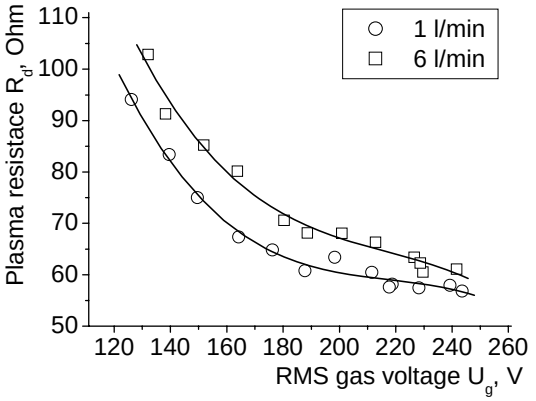

Fig. 5. Dependencies of discharge plasma resistance R_d on gas voltage U_g for different volume rates of argon flow

As it is shown above, both discharge power W_d, and gas space capacity C_g are practically independent on volume argon flow rate at its variations in range 1…6 l/min. Other kind of behavior is demonstrated by dependence of discharge plasma active resistance R_d on U_g (see Fig. 5).

Although these dependencies are qualitatively similar, resistance R_d at flow rate of 6 l/min is about 15% higher than analogous value at lower flow rate in the whole range of U_g variation. R_d growth at flow rate increase gives indirect evidence to our assumption about the role of metastable argon atoms in the ionization processes in the discharge under study.

Now let us consider current-voltage characteristics (CVC) of the discharge (Fig. 6). One can see that change of argon flow rate from 1 to 6 l/min almost have no influence on the discharge CVC. One can also see from the figure that at increase of discharge current density from ≈ 20 to 45 mA/cm^2, voltage at gas space U_g grows up practically linearly from ≈ 120 до 220 V, and after that U_g growth is considerably reduced, so that at J_d increase from 45 тодо 65 mA/cm^2 it reaches just ≈ 240 V.

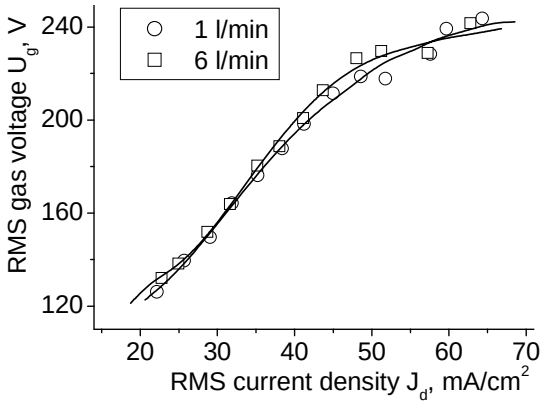

Fig .6. Dependencies of gas voltage U_g on discharge current density J_d for different volume rates of argon flow

As in case of the discharge CVC, growing dependence of the discharge gas space capacity C_g on J_d exhibits a bend at discharge current density of about 45 mA/cm^2 (Fig. 7). However, in this case, rate of C_g growth at $J_d \geq 45$ mA/cm^2 increases.

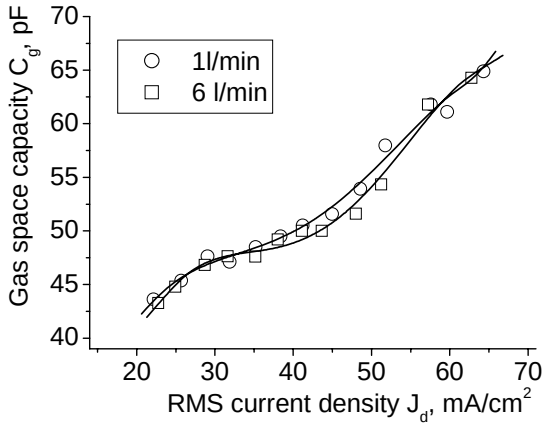

Fig. 7. Dependencies of the discharge gas space capacity C_g on discharge current density J_d for different volume rates of argon flow

Increase of argon flow rate from 1 to 6 l/min leads to R_d increase in the whole range of J_d variations. However, unlike the case of R_d dependence presented in Fig. 8, in this case for both flow rate values, discharge

active resistance is practically independent on J_d when current density is higher than about 50 mA/cm^2.

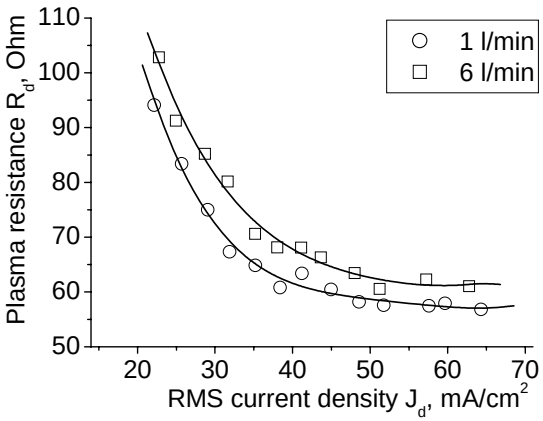

Fig. 8. Dependencies of active resistance of the discharge plasma R_d on discharge current density J_d for different volume rates of argon flow

Thus, presented results of measurements of electric characteristics of the discharge provide dual impression. On one side, abrupt growth of the discharge power W_d and gas space capacity C_g after increase of U_g and J_d above respective threshold values, undoubtedly give evidence to discharge transition from α mode to higher current γ mode. On another side, one can see from Fig. 6 that in whole range of discharge current density variations, plasma exhibits positive differential conductance. However, as it was shown in [6], RF discharge transition from α mode to γ mode should be accompanied by change of sign of plasma differential conductivity. For clarifying this issue, we have performed researches of characteristics of the discharge plasma emission.

2.2. RESULTS OF THE OPTICAL MEASUREMENTS

One can see from Fig. 9 that emission spectrum of RF discharge plasma in argon can be conditionally subdivided into two portions – emission of argon UV-VIS continuum in wavelength range ≈ 350…650 nm and emission of atomic argon spectrum lines in range ≈ 700…900 nm (mainly, it is emission of transitions $2p_{10\text{-}1}…1s_{2\text{-}5}$). The reason for appearance of emission of NOβ system is presence of air admixture coming from the walls of gas feeding tubes.

For the first time, emission of argon UV-VIS continuum in such wide range of spectrum (up to 650 nm) was discovered in [13] at study of pulsed discharge in argon at 4 bar pressure. (Emission spectrum of the continuum due to photorecombination of atomic ions Ar^+ shows sharp edge at about 460 nm). Authors of that paper supposed that on the analogy of atomic Ar^+ ions, the electron could be captured by molecular Ar^+_2 ions and transferred into Ar^*_2 energy levels with the emission of a photon: $Ar^+_2 + e \rightarrow Ar^*_2 + h\nu$.

Estimation of the plasma density was done with the use of ratios of emission intensities of transitions $2p_1$-$1s_2$, 750.4 nm; $2p_3$-$1s_4$, 738.4 nm; $2p_6$-$1s_5$, 763.5 nm by means of method proposed in [14], which has shown that plasma density in the discharge at W_d = 30 W and gas flow rate 6 l/min is ~ 10^{12} cm^{-3}.

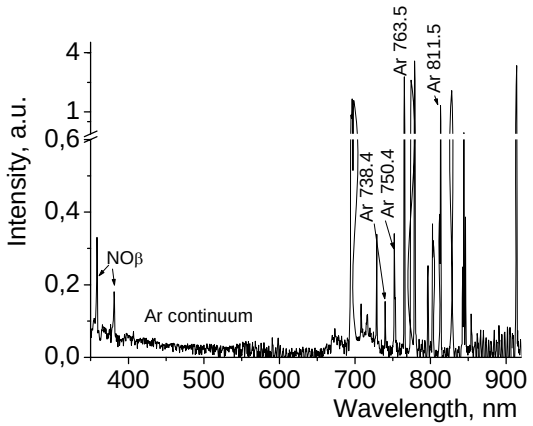

Fig .9. Emission spectrum of the discharge plasma. Argon flow rate 6 l/min, W_d = 30 W

Study of the discharge emission spatial distribution by means of long focal length optical setup described above have shown that the bend occurring in electrical characteristics of the discharge is accompanied by change of the emission profile in direction across the discharge gap – while at lower discharge power the discharge exhibited distinct dark regions near both isolator (Fig. 10, curve 1), at higher power values discharge emission had a tendency of filling the whole gap space.

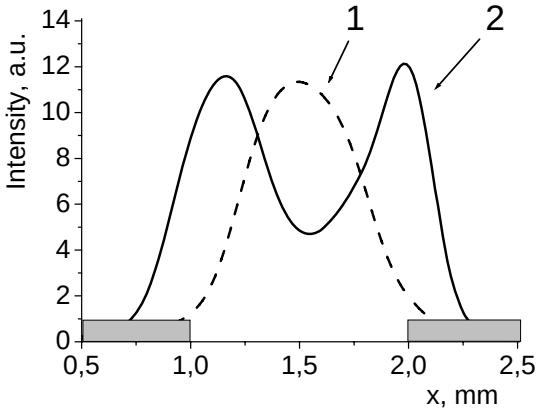

Fig. 10. Emission profiles across the discharge gap. The discharge glows in α (1) and γ (2) modes

However, it occurred only in part of the gap under center of the electrodes. By investigating the emission profiles when viewing the cell at different angles in the gap plane (up to 30^0 with respect to the axis) it was found that the discharge changes only in a spot lying exactly under center of the electrodes where power supply wires were soldered. For obtaining the discharge emission profile in the spot, calculation of intensity distribution was done, at which measured profile corresponding to the gap center was modified by partial subtraction of the profile measured outside of the spot, at that the part was defined by portion occupied by the spot along the line of view taken relatively to the whole discharge length (5 cm). Normalized resulted profile is shown in Fig. 10, curve 2. One can see two maxima spaced by about the size of the discharge gap thickness. Taking into account diffraction broadening of the image, one can state that the discharge emission occurs mainly in two regions located very close to the dielectric barriers, which gives undoubted evidence to discharge transition to γ mode in center portion of the cell. Uncontrolled variations of the size of this portion repre-

sent a reason for increased spread of electrical parameters of the discharge when it was investigated at higher power values.

Thus, the results of optical measurements have clarified the situation with the discharge transitions between glow modes. Indeed, the discharge switches from α to γ mode of glow after reaching threshold of the current density of about 45 mA/cm^2. However, γ mode discharge glow coexists with α mode one, at that the last occupies major portion of the discharge volume. As a result, in spite of higher local current density in γ mode, averaged electrical characteristics only partially resemble the switch of the discharge glow modes. Particularly, differential plasma conductivity may locally change its sign, as it is expected accordingly to [6]. Realization of uniform discharge glow in γ mode should undoubtedly improve its operation efficiency.

REFERENCES

1. R. Foest, E. Kindel, A. Ohl, M. Stieber, and K.D. Weltmann. Non-thermal atmospheric pressure discharges for surface modification // *Plasma Phys. Control. Fusion.* 2005, v. 47, p. B525-36.
2. M.G. Kong, G. Kroesen, G. Morfill, et al. Plasma medicine: an introductory review // *New J. Phys.* 2009, v. 11, p. 115012.
3. D. Janasek, J. Franzke, and A. Manz. Scaling and the design of miniaturized chemical-analysis systems // *Nature*. 2006, v. 442, № 7101, p. 374-380.
4. X. Yang. Comparison of an atmospheric pressure, radio-frequency discharge operating in the *α* and *γ* modes // *Plasma Sources Sci. Technol.* 2005, v. 14, № 2, p. 314-320.
5. S.Y. Moon, W. Choe, B.K. Kang. A uniform glow discharge plasma source at atmospheric pressure // *Appl. Phys. Let*. 2004, v. 84, № 2, p. 188-190.
6. J.J. Shi, D.W. Liu, M.G. Kong. Plasma stability control using dielectric barriers in radio-frequency atmospheric pressure glow discharge // *Appl. Phys. Let*. 2006, v. 89, p. 081502.
7. J.J. Shi, D.W. Liu, M.G. Kong. Mitigation plasma constriction using dielectric barriers in radio-frequency atmospheric pressure glow discharges // *Appl. Phys. Let*. 2007, v. 90, p. 031505.
8. J.J. Shi, D.W. Liu, M.G. Kong. Effect of dielectric barriers in radio-frequency atmospheric glow discharges // *IEEE Trans. Pl. Sci*. 2007, v. 35, № 2, p. 137-142.
9. V.Yu. Bazhenov, R.Yu. Chaplinskiy, R.M. Kravchuk, et al. Treatment of polyimide films by an atmospheric pressure plasma of capacitive RF discharge for liquid crystal alignment // *Problems of Atomic Science and Technology. Series "Plasma Physics" (19)*. 2013, № 1, p. 177-179.
10. P. McCallion, M.B. Shah and H.E. Gilbody. A crossed beam study of the multiple ionization of argon by electron impact // *J. Phys. B: At. Mol. Opt. Phys*. 1992, v. 25, p. 1061-1071.
11. M. Asgar Ali, P.M. Stone. Electron impact ionization of metastable rare gases: He, Ne and Ar // *Int. J. Mass Spectr*. 2008, v. 271, p. 51-57.
12. M.W. Kiehlbauch and D.B. Graves. Modeling argon inductively coupled plasmas: The electron energy distribution function and metastable kinetics // *J. Appl. Phys.* 2002, v. 91, № 6, p. 3539-3546.
13. A.B. Treshchalov and A. A. Lissovski. VUV–VIS spectroscopic diagnostics of a pulsed high-pressure discharge in argon // *J. Phys. D: Appl. Phys.* 2009, v. 42, 245203 (14 p.).
14. X.M. Zhu, Y.K. Pu, N. Balcon and R. Boswell. Measurement of the electron density in atmospheric-pressure low-temperature argon discharges by line-ratio method of optical emission spectroscopy // *J. Phys. D: Appl. Phys*. 2009, v. 42, 142003 (5 p.).

Article received 08.04.2013.

ОСОБЕННОСТИ РЕЖИМОВ ГОРЕНИЯ ЕМКОСТНОГО ВЫСОКОЧАСТОТНОГО РАЗРЯДА С ИЗОЛИРОВАННЫМИ ЭЛЕКТРОДАМИ В АРГОНЕ АТМОСФЕРНОГО ДАВЛЕНИЯ

В.Ю. Баженов, В.В. Циолко, В.М. Пиун, Р.Ю. Чаплинский, А.И. Кузмичев

Экспериментально установлены характеристики горения емкостного высокочастотного разряда с изолированными электродами в слаботочном (α) и сильноточном (γ) режимах. Показано, что переход из режима α в режим γ происходит через фазу одновременного существования двух режимов в разных частях разрядного промежутка.

ОСОБЛИВОСТІ РЕЖИМІВ ГОРІННЯ ЄМНІСНОГО ВИСОКОЧАСТОТНОГО РОЗРЯДУ З ІЗОЛЬОВАНИМИ ЕЛЕКТРОДАМИ В АРГОНІ АТМОСФЕРНОГО ТИСКУ

В.Ю. Баженов, В.В. Ціолко, В.М. Піун, Р.Ю. Чаплінський, А.І. Кузмічов

Експериментально встановлено характеристики горіння ємнісного високочастотного розряду з ізольованими електродами в аргоні атмосферного тиску в слабострумовому (α) та сильнострумовому (γ) режимах. Показано, що перехід з режиму α в режим γ відбувається через фазу одночасного існування двох режимів в різних частинах розрядного проміжку.